Plasma diagnostics and low-temperature deposition of microcrystalline silicon films in ultrahigh-frequency silane plasma

Shigeaki Sumiya, Yuko Mizutani, Ryohei Yoshida, Masaru Hori,[a] and Toshio Goto
Department of Quantum Engineering, Graduate School of Engineering, Nagoya University, Furocho, Chikusa-ku, Nagoya 464-8603, Japan

Masafumi Ito
Department of Opto-Mechatronics, Faculty of Systems Engineering, Wakayama University, 930 Sakaedani Wakayama, 640-8510, Japan

Tsutomu Tsukada
ANELVA cooperation, 5-8-1, Yotsuya, Fuchu-shi, Tokyo 183-8508, Japan

Seiji Samukawa
NEC cooperation, 34 Miyukigaoka, Tsukuba 305-8501, Japan

(Received 7 October 1999; accepted for publication 6 April 2000)

Microcrystalline silicon thin films were formed on quartz substrates by ultrahigh-frequency (UHF) plasma enhanced chemical vapor deposition from a mixture of silane (SiH_4) and hydrogen (H_2) gases at low substrate temperatures (T_s). The UHF plasma was excited at a frequency of 500 MHz. The deposition rate and the crystallinity of the films were investigated as a function of H_2 dilution, total pressure, mixture ratio of SiH_4 to H_2 and T_s. A crystalline fraction of 63% with a high deposition rate of 7.7 Å/s was obtained even at a T_s of 100 °C. At a temperature of 300 °C, a crystalline fraction of approximately 86% was achieved at a deposition rate of 1.4 Å/s. Diagnostics of the UHF plasma have been carried out using a Langmuir probe, ultraviolet absorption spectroscopy, and optical emission spectroscopy. Good crystallinity was explained by the balance of the sheath voltage and atomic hydrogen densities in the UHF plasma. Namely, the UHF plasma source achieving a high density plasma with a low electron temperature enabled us to reduce the ion bombardment energy incident on the substrates while maintaining a high density of hydrogen atoms, and which improved the crystallinity at low T_s. © *2000 American Institute of Physics.* [S0021-8979(00)10013-1]

I. INTRODUCTION

Microcrystalline silicon (μc-Si) thin films are attractive for use in many device applications, for example, solar cells and thin film transistors (TFTs) in liquid crystal displays, because of their high optical absorption, high carrier mobility, and stable behavior under illumination compared to amorphous silicon (a-Si). From the viewpoint of cost, high performance of the μc-Si formation process at low substrate temperatures (T_s) is required, i.e., high deposition rate and good crystallinity on inexpensive substrates such as glass substrates.

Plasma enhanced chemical vapor deposition (PECVD) is a useful method for the direct formation of μc-Si films at low T_s. The high dilution of silane (SiH_4) gas with hydrogen (H_2) gas was found to enhance the crystallization of PECVD Si films.[1–3] This is generally explained by the effect of surface coverage by hydrogen atoms,[1] the etching reaction by hydrogen atoms,[2,4,5] and/or the modification of the Si–Si network by hydrogen atoms.[6]

Furthermore, it is well known that ion bombardment does not enhance the crystallinity of μc-Si materials in PECVD.[7] Therefore, a plasma system with a high density and low electron temperature is expected to produce high quality μc-Si films with a high deposition rate. This is because the high density plasma enhances the dissociation of feed gases to generate a large number of species, and the low electron temperature reduces the ion energy incident on the substrate.

In our previous studies, an ultrahigh-frequency (UHF) plasma source with a spokewise antenna arrangement has been successfully applied to a large-scale and precise etching process at a high rate and with no damage in the fabrication of the ultralarge-scale integrated circuits.[8,9] The UHF plasma, where no magnetic field is required to maintain a high density plasma, has a great potential to achieve a high density and low electron temperature uniform to within ±5% over large areas of 30 cm diameter at a low pressure of 3 mTorr using Cl_2 plasma. In order to meet the requirements for μc-Si film formation, we have successfully employed an UHF plasma system of 500 MHz with a mixture of SiH_4 and H_2 gases for the deposition of μc-Si films on insulating quartz substrates.[10]

In this study, the crystallinity and deposition rate of films have been extensively investigated by varying the hydrogen dilution, total pressure, mixture ratio of SiH_4 to H_2 and T_s. Furthermore, we have carried out diagnostics of the plasma by Langmuir probe, ultraviolet absorption spectroscopy

[a]Electronic mail: hori@nuee.nagoya-u.ac.jp

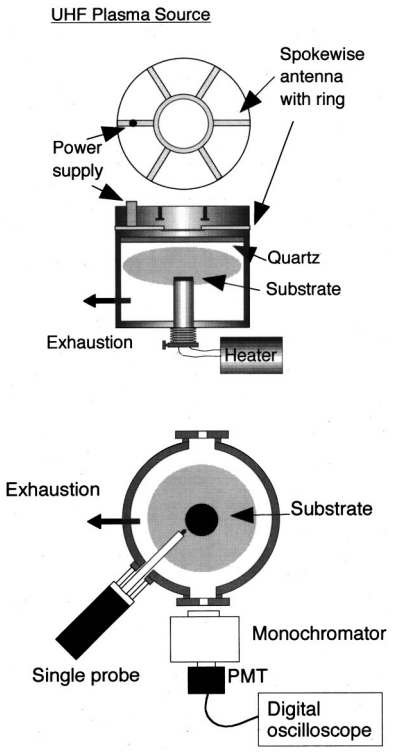

FIG. 1. Schematic illustration of the UHF plasma CVD system.

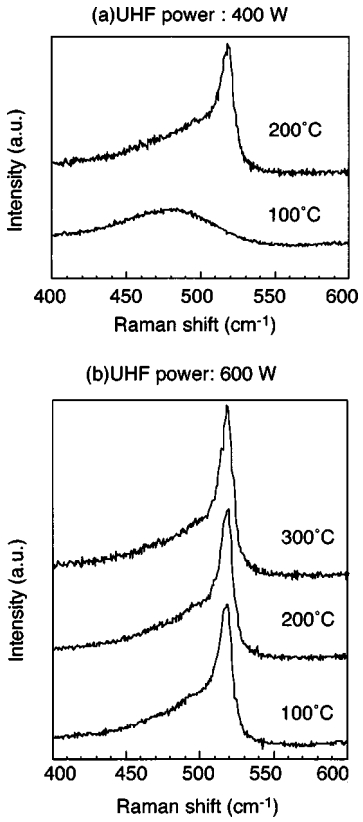

FIG. 2. Raman spectra as a function of UHF power and T_s (from 100 to 300 °C) at a pressure of 14 Pa and a SiH_4/H_2 ratio (R) of 30/100 sccm.

(UVAS), and optical emission spectroscopy (OES) to clarify the main factor determining the crystallinity in UHF plasma. On the basis of these results, the mechanism for the formation of μc-Si films with good crystallinity at low temperature employing UHF plasma is discussed.

II. EXPERIMENT

Figure 1 shows the schematic illustration of the UHF plasma CVD system. The plasma was generated by supplying an UHF power at 500 MHz to a spokewise antenna with a ring, which has been described in detail elsewhere.[11] The antenna was designed to inductively couple UHF power introduced through a 3-cm-thick quartz window. The plasma source enabled us to generate a large area of plasma (40 cm diameter) with high density ($\sim 8\times 10^{10}\,\mathrm{cm}^{-3}$) and low electron temperature at around 1 eV at 20 Pa. The process chamber was evacuated by two turbo molecular pumps (1200 and 600 l/s) and a rotary pump. A road lock chamber was arranged to introduce the substrate into the process chamber without exposing the inside of the chamber to the atmosphere. The T_s was controlled by a heater and thermocouple attached to the rear surface of the substrate. All films were deposited on the quartz substrate. We used a mixture of SiH_4 and H_2 gases and the SiH_4/H_2 ratio ranged from 0.5% to 30%. The total pressure was varied from 10 to 25 Pa. Raman spectroscopy was used to evaluate the crystallinity of deposited films. The thickness of the films for Raman spectroscopy was about 700 nm throughout the present experiments. The plasma was analyzed by Langmuir probe, UVAS, and OES. A monochromator with a wavelength resolution of 0.3 nm and a photomultiplier tube to detect the light were used for the UVAS and OES measurements. A 35 GHz microwave interferometer was used to measure the electron densities.

III. RESULTS AND DISCUSSION

Figure 2 shows Raman spectra as a function of UHF power and T_s (from 100 to 300 °C) at a pressure of 14 Pa and a SiH_4/H_2 ratio (R) of 30/100 sccm.

To evaluate the crystallinity of the films, we used the crystalline fraction assessed by decomposing the Raman spectra into three peaks, namely, crystalline (518 cm^{-1}), amorphous (480 cm^{-1}), and intermediate (512 cm^{-1}) peaks. The crystalline fraction X_c was derived from the formula as follows;

$$X_c=\frac{I_c+I_m}{I_c+I_m+\sigma I_a}, \tag{1}$$

where I_c, I_m, and I_a are the integrated intensities of the crystalline, intermediate, and amorphous peaks, respectively. σ is the ratio of the integrated Raman cross sections for amorphous silicon to that for crystalline silicon. In this analysis, we evaluated the crystalline fraction by subtracting the spectra due to the quartz substrate from the Raman spectra and the σ was assumed to be 1.[12,13]

In the case of (a) 400 W, at a T_s of 100 °C, only a broad peak near 480 cm^{-1}, arising from a-Si, was observed. At 200 °C, a peak at 518 cm^{-1} appeared arising from crystalline silicon phase. On the other hand, in the case of (b) 600 W, the peaks of the crystalline phase were obtained even at 100 °C. In this condition, the crystalline fraction and deposi-

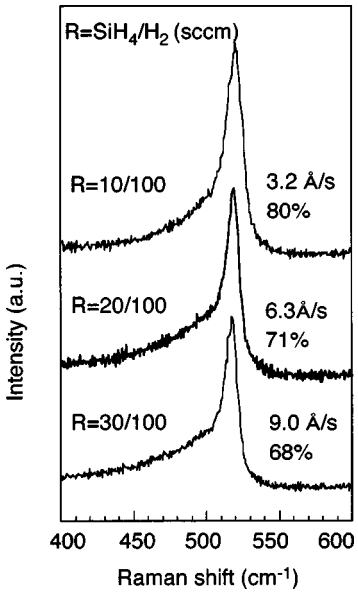

FIG. 3. Raman spectra as a function of SiH_4/H_2 dilution ratio at a fixed H_2 flow rate of 100 sccm, a T_s of 300 °C, an UHF power of 600 W, and a total pressure of 14 Pa.

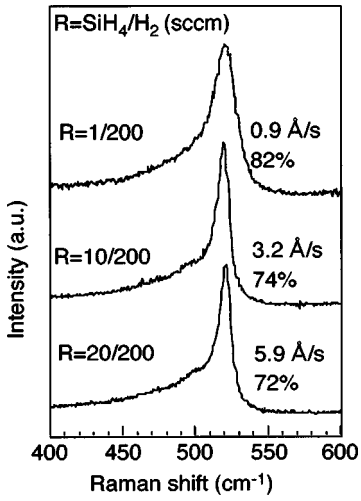

FIG. 4. Raman spectra as a function of SiH_4 flow rate and constant with H_2 flow rate at an UHF power of 600 W, a pressure of 14 Pa, and a T_s of 300 °C.

tion rate were estimated to be about 63% and 7.7 Å/s, respectively. At 300 °C, a crystalline fraction of about 68% with a deposition rate of 9.0 Å/s was obtained. We confirmed that the crystalline fractions of all the films increased with T_s. These results indicate that the SiH_4 and H_2 gases were effectively dissociated into favorable precursors and that the ion bombardment energy, which was estimated to be about 8 eV at a pressure of 14 Pa as described later, was is low enough to form the crystalline phase in the higher power region of the UHF plasma.

Figure 3 shows Raman spectra as a function of SiH_4/H_2 dilution ratio at a fixed H_2 flow rate of 100 sccm, T_s of 300 °C, UHF power of 600 W, and total pressure of 14 Pa. As the dilution ratio, $R(SiH_4/H_2)$, was varied from 30/100 to 10/100 sccm, the crystalline fraction was improved from 68% to 73%. The deposition rate decreased from 9.0 to 3.2 Å/s with decreasing the dilution ratio of SiH_4 to H_2. Figure 4 shows the Raman spectra as a function of SiH_4 flow rate at a constant H_2 flow rate, UHF power of 600 W, a pressure of 14 Pa, and a T_s of 300 °C. As the dilution ratio was varied from 20/200 to 1/200 sccm at a high flow rate condition, the crystalline fraction was improved from 72% to 82% and the deposition rate decreased from about 6 to 1 Å/s. The origin of the bump at about 500 cm^{-1} was the quartz substrate. Compared with the results of $R=10/100$ in Fig. 3 and $R=20/200$ in Fig. 4 for a constant dilution ratio of SiH_4/H_2, as the total flow rate of the gas mixture increased, the deposition rate increased from 3.2 to 5.9 Å/s, while the crystalline fraction did not change much. Therefore, the total flow rate does not affect the crystalline fraction. At these conditions, the residence times of the gas were estimated to be about 3.3 s at $R=10/100$ and 1.7 s at $R=20/200$.

Figure 5 shows the dependence of the deposition rate on the T_s at an UHF power of 600 W and pressure of 14 Pa. The deposition rates were almost constant at T_s from 100 to 300 °C and depended on the SiH_4 flow rate. Thus, the deposition rate of μc-Si films can be controlled by the SiH_4 flow rate.

Figure 6 shows the Raman spectra as a function of the total pressure at $R=1/200$ sccm and $R=1/200$ sccm of films deposited at 300 °C and 600 W. The deposition rates increased with increasing the total pressure. The crystalline fraction of films at both H_2 dilution ratios tended to decrease with an increase in the total pressure. As shown in Eq. (1), the crystalline fraction described earlier indicates the volume fraction including the crystalline and nanocrystalline components. For high quality TFTs, however, the crystalline grain size is required to be large and therefore, the crystalline component should be evaluated. The full width at half maximum (FWHM) of the crystalline component spectrum decomposed from the Raman spectra has a close relation to the grain size of the crystalline phase.[12] Namely, the lower the FWHM, the larger the grain size.

Figure 7 shows the behavior of the FWHM as the total pressure was varied at 600 W and 300 °C. From these results, the grain sizes of films deposited at $R=1/200$ sccm and $R=10/200$ sccm have the maximum values of about 14 and 20

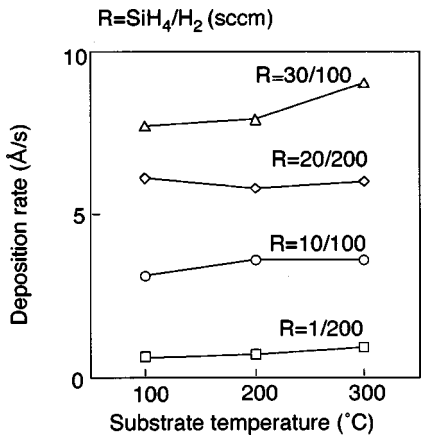

FIG. 5. Dependence of the deposition rate on the T_s at an UHF power of 600 W at a pressure of 14 Pa.

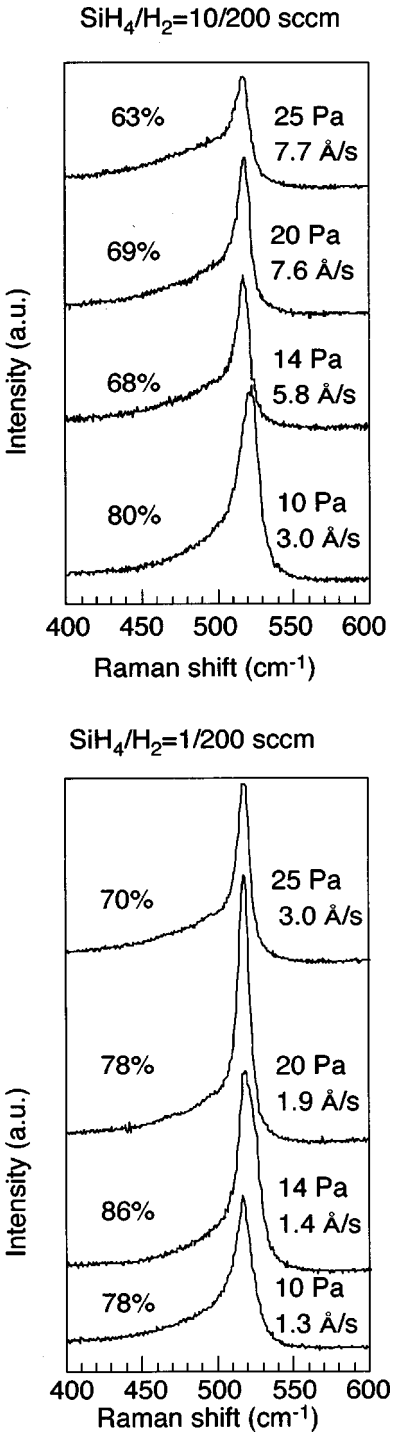

FIG. 6. Raman spectra as a function of the total pressure for hydrogen dilution ratios of $R=1/200$ sccm sccm and $R=10/200$ sccm at 300 °C and 600 W.

Pa, respectively. The crystalline grain size estimated by x-ray diffraction showed the same trend as the FWHM obtained by Raman spectroscopy. The formations of these films were randomly oriented textures and the crystalline grain size at $R=1/200$ and 20 Pa was about 25 nm. The deposition rates and crystalline fractions estimated from the Raman spectra of these films were 1.9 Å/s and 78% at $R=1/200$, 5.8 Å/s and 68% at $R=10/200$, respectively.

To clarify these behaviors, we initially obtained information about the plasmas using OES. In OES measurements, small amounts of the rare gases He, Ar, and Xe were added to the SiH_4/H_2 plasmas. The optical emission intensity of Ar is given

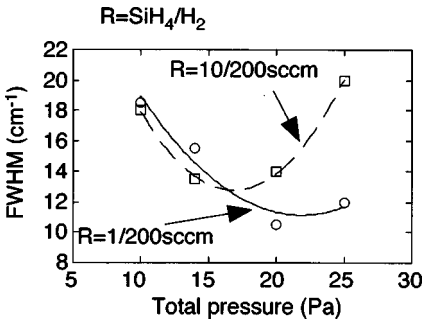

FIG. 7. FWHM of the crystalline component estimated from the Raman spectra in Fig. 6 for a variety of total pressure.

$$I_{\mathrm{Ar}*} \propto n_e N(\mathrm{Ar}) \int_{\epsilon_{\mathrm{th}}}^{\infty} \nu(\epsilon)\sigma(\epsilon) f(\epsilon) d\epsilon = n_e N(\mathrm{Ar}) \langle \sigma\nu \rangle, \tag{2}$$

where n_e is the electron density, $N(\mathrm{Ar})$ is the density of Ar, $\nu(\epsilon)$ is the electron velocity as a function of electron energy ϵ, $\sigma(\epsilon)$ is the collisional cross section for the electron impact excitation of Ar, and $f(\epsilon)$ is the electron energy distribution function (EEDF). The emission rate, i.e., the integral term, is simplified by the symbol $\langle \sigma\nu \rangle$. Figure 8 shows the normalized optical emission intensity of Ar $[I_{\mathrm{Ar}*}/N(\mathrm{Ar})]$ and the optical emission intensity ratios of Xe/Ar and He/Ar for $R=1/200$ and Xe/Ar (He/Ar)=1/1 sccm. The lines used were Xe ($5p^5 6s\, 3P - 5p^5 6p\, 1P$: 823.1 nm),[14] Ar ($1s2-2p1$: 750.4 nm),[15] and He ($1s2p\,{}^3P^0 - 1s3d\,{}^3D$: 587.6 nm) and their excitation threshold energies were 9.8, 13.5, and 23.1 eV, respectively. These optical emissions were caused by electrons with higher energies than the threshold values. The Xe/Ar ratio increased while the He/Ar ratio decreased with increasing the total pressure. Xe/Ar indicates the lower energy distribution region while He/Ar indicates the higher region. This fact indicates that the EEDF in the plasma shifts to the lower energy region with increasing total pressure. Moreover, $I_{\mathrm{Ar}*}/N(\mathrm{Ar})$ decreased with increasing the total pressure and $I_{\mathrm{Ar}*}/N(\mathrm{Ar})$ is proportional to $n_e\langle \sigma\nu \rangle$. Hence, the decrease in $I_{\mathrm{Ar}*}/N(\mathrm{Ar})$ means a decrease in $n_e\langle \sigma\nu \rangle$. The electron density n_e was evaluated using a microwave

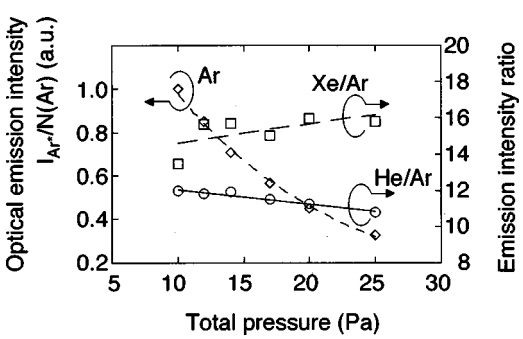

FIG. 8. Normalized optical emission intensity of Ar and emission intensity ratio of Xe/He and He/Ar.

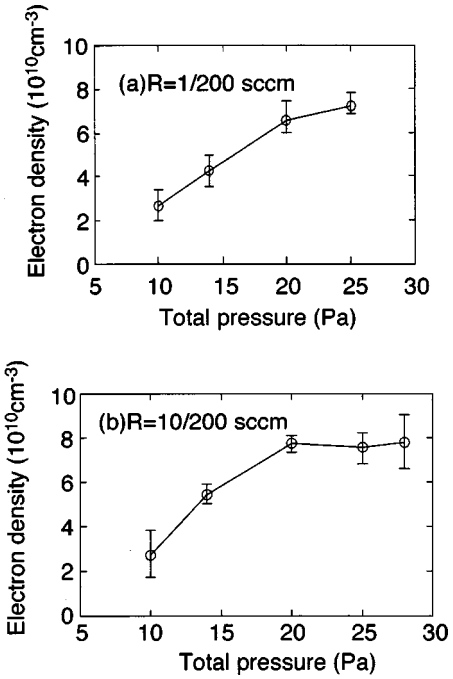

FIG. 9. Dependence of the electron density measured by a microwave interferometer on the total pressure at (a) $R=1/200$ sccm and (b) $R=10/200$ sccm.

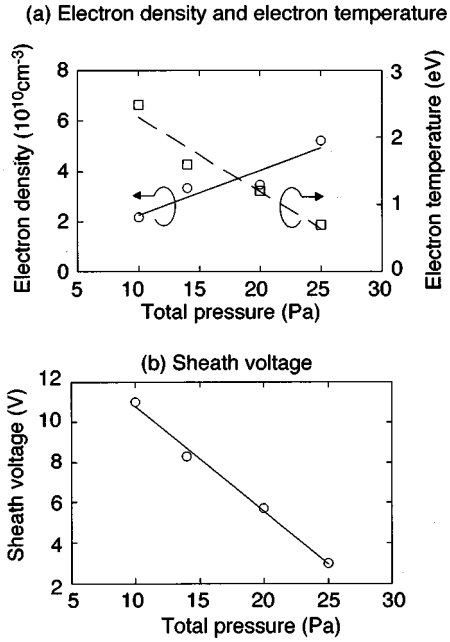

FIG. 10. (a) The electron density and electron temperature, and (b) the sheath voltage estimated by using the probe method as a function of the total pressure.

interferometer. Figure 9 shows the dependence of electron density on the total pressure at an UHF power of 600 W. As shown in Fig. 9, the electron density n_e increased with the total pressure and had a tendency to become saturated at pressures greater than 20 Pa in both the cases of $R=SiH_4/H_2=1/200$ and $R=10/200$. Almost identical electron densities were achieved for at $R=1/200$ and $R=10/200$ because the plasmas in both cases consisted of over 95% H_2.

In a previous study, the ionization rate was characterized in UHF and inductively coupled plasmas (ICPs) employing Cl_2 gas. It was found that the ionization rate in the UHF plasma remained high compared with the rate in the ICP with a discharge frequency of 13.56 MHz and at low pressure, whereas the rate in the ICP fell sharply as the pressure increased.[16,17] These results were explained by the relationship between the discharge frequency and the electron-collision frequency, namely, the discharge frequency in the UHF plasma is higher than the collision frequency in the pressure region and thus the electron energy distributions are insensitive to the variation in pressure. Moreover, the ionization rate in the UHF plasma employing Cl_2 gas increased up to about 20 Pa and was almost constant with increasing the pressure.[18] The results in the UHF plasma employing a mixture of SiH_4 and H_2 gases, shown in Fig. 9, are reasonably consistent with those employing Cl_2 gas obtained in the previous studies. Therefore, these results indicate the specific feature of UHF plasma where the density remains high compared with other plasmas, such as ICP, not only in the low-pressure region but also in the high-pressure region from 10 to 25 Pa.

$n_e\langle\sigma\nu\rangle$ decreased while n_e increased. Therefore, $\langle\sigma\nu\rangle$ decreases with increasing total pressure. The ion bombardment energy to the floating substrate is generally a function of $\langle\sigma\nu\rangle$. Therefore, the ion bombardment energy incident on the film surface is considered to be lower with increasing total pressure. To confirm the decrease of the sheath voltage, the Langmuir probe method was also carried out. These measurements were only performed for H_2 flow rate of 200 sccm and without SiH_4 gas in order to avoid the problem of contamination on the probe in the plasma. The sheath voltage was estimated from V_s-V_f, where the V_f is the floating potential and the V_s is the space potential. Figure 10 shows the electron density, electron temperature, and sheath voltage estimated by using the probe method as a function of the total pressure at 600 W. The sheath voltage decreased with increasing total pressure. Moreover, we confirmed that the electron temperature T_e decreased with increasing total pressure. The electron temperatures were derived to be 1.2 eV at 20 Pa and 0.7 eV at 25 Pa, which indicated well the characteristics of UHF plasmas with a high density and a low electron temperature. Consequently, the main factor for improving the crystallinity evaluated from the FWHMs of the crystalline component is considered to be the reduction in the ion bombardment energy. However, the crystallinity has an optimum pressure as shown in Fig. 7. This fact means that there are factors for deteriorating the crystallinity.

Many studies have reported that hydrogen atoms play an important role for improving crystallinity. In order to investigate this further, the behavior of atomic hydrogen and the species for deposition were studied by OES and UVAS were carried out. In this study, we investigated the density of atomic silicon as one of the deposition species. The UVAS measurement, using a silicon hollow cathode lamp as the light source, was used to measure the absolute densities of the atomic silicon in the gas phase.[19,20] The transition $3p^2\,{}^2P_2-3p4s\,{}^3P_2$ line of atomic silicon atom at 251.6 nm was used for the measurement. On the other hand, no simple

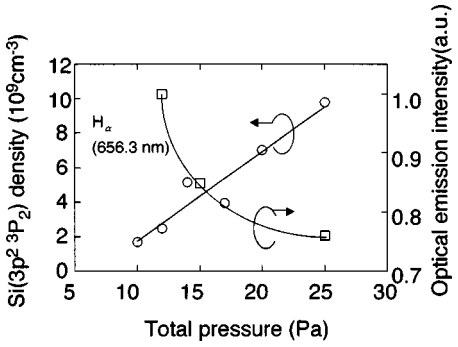

FIG. 11. Silicon density ($3p^2\,{}^2P_2-3p4s\,{}^3P_2$) and the optical emission intensity of H_α (656.3 nm) as a function of the total pressure at $R=1/200$ sccm.

measurement method has been established for obtaining the absolute density of atomic hydrogen. Hence, OES was employed to estimate the behavior of the relative densities of atomic hydrogen.

In the SiH_4 plasma highly diluted by H_2 gas, the optical emission (e.g., H_α) is considered to be mainly due to the dissociative emission from H_2 molecules and excitation of H atoms.[21] Thus, the optical intensity indicates the production rate of hydrogen atoms. Figure 11 shows the silicon density and the optical emission intensity of H_α (656.3 nm) as a function of the total pressure at $R=1/200$ sccm and 600 W. From the intensity of H_α, hydrogen atoms in the plasma seem to decrease with increasing total pressure. This agrees with the result that electrons with high energy, probably dissociate H_2 molecules, decrease with increasing total pressure as discussed in Fig. 8. The number of silicon atoms increased with increasing the total pressure. This indicates that the species for deposition still increase with pressure although the production rate of $n_e\langle\sigma\nu\rangle$ decreases. Consequently, the decrease in the ratio of atomic hydrogen density to the deposition species is considered to be the main reason for deterioration of the crystallinity. For the $R=10/200$ result, the optimum pressure is considered to lower compared with the $R=1/200$ result, because of the increase in the deposition species compared to hydrogen atoms.

From these results, it was found that good crystallinity is explained by the balance of the sheath voltage, that is, the ion incident energy, and the ratio of hydrogen atoms to the deposition species in UHF plasma. The reduction of the sheath voltage with increasing ratio of hydrogen atoms to deposition species was considered to be a key factor for improving the crystallinity at low T_s. Therefore, this UHF plasma source will provide a promising process for synthesizing good quality μc-Si films with high deposition rates at low T_s.

IV. CONCLUSIONS

In this study, we have employed an UHF plasma system of 500 MHz using a mixture of SiH_4 and H_2 gases to deposit μc-Si films at low temperatures from 100 to 300 °C. The deposition rate was controlled by the SiH_4 flow rate and the crystalline fraction increased with increasing H_2 dilution ratio. A crystalline fraction of 63% with a high deposition rate of 7.7 Å/s was obtained even at a of 100 °C. At a temperature of 300 °C, a crystalline fraction of approximately 86% was achieved at a deposition rate of 1.4 Å/s. Moreover, it was clarified that the electron density was constant against a variation of pressures around 25 Pa and an optimum pressure for crystallinity existed. This was explained from the viewpoint of atomic hydrogen and sheath voltage. From plasma diagnostic tests using a Langmuir probe, UVAS, and OES, it was found that the reduction in the sheath voltage with increasing the atomic hydrogen density to deposition species was a key factor for improving the crystallinity at low T_s. The UHF plasma excited at 500 MHz was able to produce a low-electron temperature and high density over a wide pressure range and an excellent plasma uniformity over a large area. Thus, UHF PECVD will be very useful for the low-temperature formation of μc-Si films with good crystallinity and high deposition rates on insulated substrates over large areas.

ACKNOWLEDGMENTS

The authors would like to thank Dr. Mineo Hiramatsu (Meijo University) for the use of the Raman spectroscopy system and Yukito Nakagawa (ANELVA Co.) for advising the UHF plasma. This work was supported by a Grant-in-Aid for Scientific Research from the Ministry of Education, Science, Sports and Culture, Japan.

[1] A. Matsuda, J. Non-Cryst. Solids **59&60**, 767 (1983).
[2] C. C. Tsai, G. B. Anderson, R. Thompson, and B. Wacker, J. Non-Cryst. Solids **114**, 151 (1989).
[3] M. Mohri, H. Kakinuma, and T. Tsuruoka, IEICE Trans. Electron. **E–77C**, 1677 (1994).
[4] S. Kumar, B. Drévillon, and C. Godet, J. Appl. Phys. **60**, 1542 (1986).
[5] R. Nozawa, H. Takeda, M. Ito, M. Hori, and T. Goto, J. Appl. Phys. **85**, 1172 (1999).
[6] I. Solomon, B. Drévillon, H. Shirai, and N. Layadi, J. Non-Cryst. Solids **164**, 989 (1993).
[7] R. Nozawa, H. Takeda, M. Ito, M. Hori, and T. Goto, J. Appl. Phys. **81**, 8035 (1997).
[8] S. Samukawa, Appl. Phys. Lett. **67**, 1414 (1995).
[9] S. Samukawa, Y. Nakagawa, T. Tsukada, H. Ueyama, and K. Shinohara, Jpn. J. Appl. Phys., Part 1 **34**, 6805 (1995).
[10] B. Mebarki *et al.*, Mater. Lett. **41**, 16 (1999).
[11] Y. Nakagawa, E. Wani, K. Takagi, S. Samukawa, K. Shinohara, H. Ueyama, H. Sato, and T. Tsukada, Dig. Microprocesses and Nanotechnol. '97, Nagoya (1997), Vol. 56.
[12] Z. Iqbal and S. Veprek, J. Phys. C **15**, 377 (1982).
[13] T. Kaneko, K. Onisawa, M. Wakagi, Y. Kita, and T. Minemura, Jpn. J. Appl. Phys., Part 1 **32**, 4907 (1993).
[14] P. K. Janev, W. E. Kanger, K. Evans, Jr., and D. E. Post; *Elementary Processes in Hydrogen*–Helium Plasmas (Springer, Berlin, 1987).
[15] C. F. Barnett *et al.*, Atomic Data for Controlled Fusion Research (1977).
[16] H. Akashi and S. Samukawa, Jpn. J. Appl. Phys., Part 2 **36**, L877 (1997).
[17] S. Samukawa and H. Akashi, IEEE Trans. Plasma Sci. **26**, 1621 (1998).
[18] H. Akashi, S. Samukawa, N. Takahashi, and T. Sasaki, Program of the 50th Annual Gaseous Electronics Conference (1997), Vol. 42, p. 1744.
[19] M. Sakakibara, M. Hiramatsu, and T. Goto, J. Phys. D **15**, 177 (1982).
[20] Y. Yamamoto, H. Nomura, T. Tanaka, M. Hiramatsu, M. Hori, and T. Goto, Jpn. J. Appl. Phys., Part 1 **33**, 4320 (1994).
[21] V. Schulz-von der Gathen and H. F. Dobele, Plasma Chem. Plasma Process. **16**, 461 (1996).